

Paramagnetic Resonance and Relaxation of Trivalent Rare-Earth Ions in Calcium Fluoride. I. Resonance Spectra and Crystal Fields

M. J. WEBER AND R. W. BIERIG

Raytheon Research Division, Waltham, Massachusetts

(Received 3 January 1964)

The energy level structures arising from the crystal-field splitting of the free-ion ground states of trivalent rare-earth ions in CaF_2 are determined from a survey of the optical and electron paramagnetic resonance spectra. The predicted ground states are in agreement with existing paramagnetic resonance data. Estimates are made of the magnitude of the cubic crystal-field parameters and their variation throughout the rare-earth series. Axial crystal fields of tetragonal and trigonal symmetries, due to nearest-neighbor charge compensation, are found to cause large perturbations on the cubic-field energy levels. The paramagnetic resonance spectra of all rare-earth ions are reviewed and new resonances for Ce^{3+} , Sm^{3+} , Er^{3+} , and Yb^{3+} are reported. Expressions for the calculation of crystal-field matrix elements in terms of $3-j$ and $6-j$ symbols and their relationship to the operator equivalent approach are given in an Appendix.

INTRODUCTION

RARE-EARTH ions of the lanthanide series can be introduced into a calcium fluoride host lattice substitutionally at divalent calcium sites. Although several of the rare earths can be stabilized in the divalent state in alkaline earth halide lattices, we shall be concerned almost exclusively with the trivalent rare-earth ions. In the case of the trivalent rare earths, a question arises regarding the compensation of the additional positive charge associated with a trivalent ion substituted in a divalent site. Several different charge compensation mechanisms have been found in CaF_2 which depend upon the growth conditions, impurity concentrations, and thermal treatments of the sample. The crystalline electrostatic fields at the rare-earth sites have correspondingly different magnitudes and symmetries. In this paper and the one to follow¹ (henceforth denoted as II), the electron paramagnetic resonance and spin-lattice relaxation properties of rare-earth ions in sites of different crystal-field symmetries will be examined and compared.

The interpretation of the spin-lattice relaxation results in II requires knowledge of the strength of the crystal fields, the energy level structure of the resonant ion, and the wave functions of the lower states. Unfortunately, such information for the trivalent rare-earth series in CaF_2 is still incomplete. We have made estimates of the cubic crystal-field parameters, their variation throughout the lanthanide series, and the relative size and effect of axial field perturbations from a survey of available optical spectra of rare-earth ions in CaF_2 . This information, while not precise, is nevertheless valuable in analyzing paramagnetic resonance spectra, calculating the magnitude of spin-lattice coupling, and estimating the crystal-field splittings when direct measurements are lacking. The predicted crystal-field splittings, ground state, and excited states of the lowest J multiplet of rare earths in various symmetry sites are correlated with the findings of paramagnetic resonance

studies. For this purpose a review of the paramagnetic resonance spectra is made which will also provide a basis for the discussion of the relaxation properties of the ions in II.

CHARGE COMPENSATION AND CRYSTAL-FIELD SYMMETRY

Calcium fluoride has the fluoride structure with O_h ⁵ space group symmetry. This may be visualized as a cubic lattice of fluorine ions in which every other body-center position is occupied by a divalent calcium ion. Rare-earth ions can enter the lattice substitutionally at Ca^{2+} sites. At such sites divalent rare-earth ions experience a cubic crystalline electric field of 8-fold fluorine coordination. Trivalent rare earths, however, experience crystal fields of differing strengths and symmetries depending upon how and where the additional positive charge is compensated. The occurrence of the different charge compensation mechanisms is dependent upon many factors associated with the total crystal growth process. Several resultant distributions of ions which generate crystal-field environments of cubic, tetragonal, trigonal, and orthorhombic symmetry are described

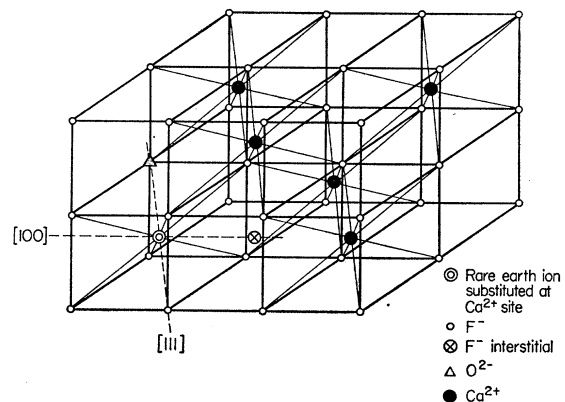


FIG. 1. A portion of the CaF_2 lattice showing the site of substitutional trivalent rare-earth ions and locations of charge compensating ions.

¹ R. W. Bierig, M. J. Weber, and S. I. Warshaw, Phys. Rev. **134**, A1504 (1964).

below and can be visualized by inspection of the CaF_2 lattice shown in Fig. 1.

The most commonly found trivalent rare-earth site in CaF_2 is one of tetragonal (C_{4v}) crystal-field symmetry. Charge compensation is attained by the presence of an F^- ion in one of the six nearest-neighbor interstitial sites at a distance $a/2=2.73 \text{ \AA}$, where a is the lattice constant. The three crystal-field symmetry axes are the $[100]$ crystallographic directions. This charge compensating mechanism has been well substantiated from investigations of density and lattice constants by x-ray methods,^{2,3} ionic conductivity,⁴ as well as by the early paramagnetic resonance results of Bleaney *et al.*⁵ and others.⁶

Paramagnetic resonance spectra exhibiting cubic symmetry are observed when charge compensation is not achieved locally. Since the excess F^- in the interstitial site is not tightly bound to the rare earth, it can diffuse through the crystal at high temperatures.⁴ Friedman and Low⁷ have used this mobility to convert from tetragonal to cubic sites. The sample is heated to disorder the rare-earth $-\text{F}^-$ pairs and then rapidly quenched. Whether the interstitial fluorine can diffuse to an energetically favorable site near a trivalent rare-earth ion or gets trapped elsewhere in the lattice depends upon the rate of cooling. Trivalent rare-earth ions of the second half of the $4f^n$ shell have been found in sites of cubic symmetry more frequently than ions of the first half. The stability of the former in cubic sites may be associated with their smaller ionic radii and different local distortions.

A crystal field of trigonal symmetry (C_{3v}) arises from the replacement of one of the eight nearest-neighbor F^- at a distance $\sqrt{3}a/4=2.36 \text{ \AA}$ by O^{2-} , a mechanism discussed by Feofilov.^{8,9} The symmetry axes are the four $[111]$ cube-body diagonals. The formation of this type of site is a function of the oxidation-reduction conditions during growth. Sierro^{10,11} has studied the effects of thermal treatment and hydrolysis at high temperatures on the trigonal resonance spectra of rare earths in alkaline earth halides. If samples are heated in an atmosphere containing a small amount of water vapor, H_2O molecules dissociate at the surface, OH^- replacing F^- which goes off as HF . Trigonal spectra corresponding to OH^- substituted for F^- have been observed. With further

thermal treatment, OH^- dissociates, the resulting O^{2-} diffusing through the crystal to compensate a trivalent rare-earth ion as above.

A paramagnetic resonance spectrum having trigonal symmetry has been observed^{12,13} from U^{4+} in CaF_2 , which is attributed to the replacement of two F^- ions at opposite corners of the fluorine cubic by two O^{2-} ions. Although a resonance from a lanthanide series ion in a similar site has not been reported, Ce, Pr, and Tb are known to exhibit tetravalent states.^{14,15}

Recently an orthorhombic spectrum of U^{3+} in CaF_2 has been reported by Mahlab *et al.*¹⁶ The X - Y axes are in a (110) plane, the X axes being at an angle of 19° with respect to $[110]$. There are twelve inequivalent magnetic sites. Several models for the charge compensation are suggested, the most likely one being an F^- in a fourth nearest-neighbor interstitial site.

In addition to lines which can be explained by the above charge compensation mechanisms, other lines have appeared in both the optical and paramagnetic resonance spectra of rare-earth ions in CaF_2 , particularly at higher rare-earth impurity concentrations. From an inspection of Fig. 1, it is not difficult to conjure up other charge compensating ion distributions at sites more distant than described above which may possibly produce measurable deviations from cubic-field symmetry. For example, F^- ions in second nearest-neighbor interstitial sites could produce a $[111]$ trigonal spectrum. [*Note added in proof.* Such trigonal spectra have been reported for Yb^{3+} in SrF_2 and BaF_2 by U. Ranon and A. Yaniv, *Phys. Letters* **9**, 17 (1964).] The replacements of two Ca^{2+} ions by a trivalent rare earth and a monovalent impurity,¹⁷ or three Ca^{2+} ions by two trivalent rare-earth ions have been suggested.¹⁸ The appearance of many new lines as the rare-earth concentration is increased may be due to the presence of energetically favored pairs or clusters of ions. Some of the lines may also be associated with other impurity ions or crystal defects.

Rare-earth-doped, alkaline earth halides exhibit additional interesting properties. For example, several trivalent rare-earth impurities have been converted to divalent ions by exposure to ionizing radiation,^{15,19-21} the resulting divalent ion being in a field of cubic sym-

² E. Zintl and A. Udgard, *Z. Anorg. Chem.* **240**, 150 (1939).

³ R. W. M. D'Eye and F. S. Martin, *J. Chem. Soc.* **349**, 1847 (1957).

⁴ R. W. Ure, *J. Chem. Phys.* **26**, 1363 (1957).

⁵ B. Bleaney, P. M. Llewellyn, and D. A. Jones, *Proc. Phys. Soc. (London)* **B69**, 858 (1956).

⁶ J. M. Baker, W. Hayes, and M. C. M. O'Brien, *Proc. Roy. Soc. (London)* **A254**, 273 (1960).

⁷ E. Friedman and W. Low, *J. Chem. Phys.* **33**, 1275 (1960).

⁸ P. P. Feofilov, *Dokl. Akad. Nauk SSSR* **99**, 731 (1954).

⁹ I. V. Stepanov and P. P. Feofilov, *Dokl. Akad. Nauk SSSR* **108**, 615 (1957) [English transl.: *Soviet Phys.—Doklady* **1**, 350 (1957)].

¹⁰ J. Sierro, *J. Chem. Phys.* **34**, 2183 (1961).

¹¹ J. Sierro, *Phys. Letters* **4**, 178 (1963).

¹² R. S. Title, P. P. Sorokin, M. J. Stevenson, G. D. Pettit, J. E. Scardefield, and J. R. Lanekard, *Phys. Rev.* **128**, 62 (1962).

¹³ A. Yariv, *Phys. Rev.* **128**, 1588 (1962).

¹⁴ F. H. Spedding, *International Science and Technology*, No. 4, 39 (1962).

¹⁵ W. Low and U. Ranon, *Paramagnetic Resonance* (Academic Press Inc., New York, 1963), p. 167.

¹⁶ E. Mahlab, V. Volterra, W. Low, and A. Yariv, *Phys. Rev.* **131**, 920 (1963).

¹⁷ B. Bleaney, *J. Appl. Phys.* **33**, Suppl. I, 358 (1962).

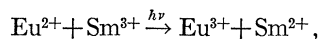
¹⁸ N. Rabbiner, *Phys. Rev.* **130**, 502 (1963).

¹⁹ W. Hayes and J. W. Twidell, *J. Chem. Phys.* **35**, 1521 (1961).

²⁰ W. Hayes, G. D. Jones, and J. W. Twidell, *Proc. Phys. Soc. (London)* **81**, 371 (1963).

²¹ W. Hayes and J. W. Twidell, *Proc. Phys. Soc. (London)* **82**, 330 (1963).

metry. Observations²² of optical absorption and conductivity due to free electrons in single crystals of CdF_2 doped with rare earths indicate charge compensation by means of electrons in conduction bands or shallow traps. Recently, optical detection of phototransfer of electrons in (Sm, Eu) doped CaF_2 of the form,



has been reported²³ and interpreted as due to electrons localized at vacancies in the vicinity of the trivalent rare earth. Photoconductivity of divalent rare-earth-doped CaF_2 has also been studied.²⁴

CRYSTAL-FIELD PARAMETERS

Information about the crystalline electric field splitting of the free-ion states can usually be derived from studies of optical absorption and fluorescence spectra. For the trivalent rare-earth series in CaF_2 , such data is in general incomplete, widely scattered, and a detailed interpretation frequently lacking or not warranted. Among the factors contributing to this status^{25,26} are that the spectra are complicated due to the presence of vibrational satellite lines, complex structure appears at moderate-to-high impurity concentrations, different types of spectra exist which are sensitive to changes in neighboring ion distributions and growth conditions, the centroids of crystal-field levels from a given state for different point symmetries do not coincide, the spectral intensities may be weak, and there is no polarized absorption to aid in the identification of cubic-field energy levels.^{27,28}

The determination of crystal-field parameters from optical data requires that the site symmetry and energy level assignments be established. Subsequent fitting procedures and numerical computations employed to obtain consistent and meaningful parameters are frequently nontrivial for the multilevel rare-earth energy structures. It may be necessary to include crystal-field admixing between states of different quantum number J and the breakdown of ideal Russell-Saunders coupling. Such detailed calculations are, with a few possible exceptions, not warranted for rare earths in CaF_2 , since much of the published data is not complete and the site symmetries are not well established. We shall therefore

content ourselves in the next section with less refined estimates of the crystal-field parameters.

The optical spectra of several divalent rare-earth ions in cubic sites in CaF_2 have been studied. Although the crystal-field parameters for these ions will differ from those of their isoelectronic trivalent neighbor, due principally to the influence of the larger effective nuclear charge, they can be of value if a suitable correlation can be found. Since some empirically derived guidance is available for extrapolating the crystal-field parameters of a divalent ion to the corresponding isoelectronic trivalent ion, we shall include several divalent ions in the survey of optical spectra.

Crystal-field parameters can also be obtained from analysis of such factors as the g values, g -value shifts, and hyperfine constants observed in paramagnetic resonance experiments.²⁹ The results, however, are in general quite sensitive to the accuracy of the measurements; for example, a small uncertainty in g value can give rise to a large variation in the derived crystal-field parameters. We shall be interested principally in a qualitative correlation between paramagnetic resonance data and the crystal-field parameters determined from optical spectra.

The Hamiltonians describing the crystal-field potentials of cubic, tetragonal, and trigonal symmetry may be written as

$$\mathcal{H}_{\text{cubic}} = B_4(O_4^0 + 5O_4^4) + B_6(O_6^0 - 21O_6^4), \quad (1)$$

where $B_4^4 = 5B_4^0$, $B_6^4 = -21B_6^0$,

$$\mathcal{H}_{\text{tetra}} = B_2^0 O_2^0 + B_4^0 O_4^0 + B_4^4 O_4^4 + B_6^0 O_6^0 + O_6^4 O_6^4, \quad (2)$$

and

$$\mathcal{H}_{\text{trig}} = B_2^0 O_2^0 + B_4^0 O_4^0 + B_4^3 O_4^3 + B_6^0 O_6^0 + B_6^3 O_6^3 + B_6^6 O_6^6. \quad (3)$$

The parameters B_n^m are related to the strength of the crystal-field components and, in the notation of Elliott and Stevens,³⁰ are equal to $\zeta_n A_n^m \langle r^n \rangle$, where ζ_n is the operator equivalent factor, α , β , γ for $n=2, 4, 6$, respectively. The O_n^m 's are angular momentum operators transforming as the corresponding spherical harmonics.

In a very useful paper, Lea, Leask, and Wolf³¹ (henceforth referred to as LLW) have determined the eigenfunction and eigenvalue solutions of Eq. (1) for various angular momentum J . Their diagrams of the eigenvalues are plotted as a function of a quantity x defined by

$$\frac{x}{1-|x|} = \frac{F(4)B_4}{F(6)B_6} = \frac{F(4)\beta A_4 \langle r^4 \rangle}{F(6)\gamma A_6 \langle r^6 \rangle}, \quad (4)$$

²² W. Low, in *Solid State Physics*, edited by F. Seitz and D. Turnbull (Academic Press Inc., New York, 1960), Suppl. 2.

²³ R. J. Elliott and K. W. H. Stevens, Proc. Roy. Soc. (London) **A218**, 553 (1953).

²⁴ K. R. Lea, M. J. M. Leask, and W. P. Wolf, Phys. Chem. Solids **23**, 1381 (1962).

²² J. D. Kingsley and J. S. Prener, Phys. Rev. Letters **8**, 315 (1962).

²³ P. P. Feofilov, Opt. i Spektroskopiya **12**, 531 (1962) [English transl.: Opt. Spectry. (USSR) **12**, 296 (1962)].

²⁴ C. H. Anderson and Z. J. Kiss, Bull. Am. Phys. Soc. **9**, 87 (1964).

²⁵ Feofilov, in a recent survey paper (Ref. 26) on luminescence of rare-earth ions in alkaline earth halides, suggested that a previous assertion may again be *à propos*, namely, that "the variability and diversity of the spectral fine structure exhibited by many phosphors with line spectra led us to the conclusion that a general individual spectra cannot serve as the basis for interpretation."

²⁶ P. P. Feofilov, Bull. Acad. Sci., USSR **26**, 437 (1962).

²⁷ Z. J. Kiss, J. Chem. Phys. **38**, 1476 (1963).

²⁸ W. Low, *Advances in Quantum Electronics* (Columbia University Press, New York, 1961), p. 138.

where $-1 < x < 1$ and the F 's are multiplicative factors given by LLW. The ordering of states within a J manifold is dependent upon the ratio of the fourth- and sixth-order cubic-field parameters B_4/B_6 , and hence from Eq. (4) upon x . The free-ion ground states of the trivalent rare earths and their decomposition in a cubic field are given in Table I. Also listed are estimated x values obtained using approximate cubic-field parameters for CaF_2 and their variation throughout the rare-earth series, which are discussed later. The predicted or experimentally observed cubic field ground states are given in the final column of Table I.

The determination of the parameters $A_n^m(r^n)$ requires the evaluation of various crystal-field matrix elements. This may be performed easily for the lowest LSJ state using the "operator equivalent" approach of Stevens³² and existing tables of matrix elements; however, when treating the crystal-field splitting of excited states $L'S'J'$ and matrix elements between different J states, it is convenient to use a more general approach which utilizes the tabulated $3-j$ and $6-j$ symbols.³³ This approach and its relationship to that of operator equivalence are developed in the Appendix. A formula is also given, in terms of $6-j$ symbols, which relates the operator equivalent factors for two different J states. Thus, given x for a state J , it can be used together with Eq. (4) to derive x for other states J' , and thereby, from LLW, the expected ordering of levels.

TABLE I. Crystal-field splitting of the free-ion ground state of trivalent rare-earth ions in a cubic field in CaF_2 . The x values are obtained using estimated crystal-field parameters in Eq. (4). * denotes ground state based upon estimated x value.

Rare-earth ion	Configuration ground state	Decomposition in cubic field	Estimated x value	Lowest state in CaF_2
Ce ³⁺	$4f^1, {}^2F_{5/2}$	$\Gamma_7 + \Gamma_8$	1.0	Γ_8
Pr ³⁺	$4f^2, {}^3H_4$	$\Gamma_1 + \Gamma_3 + \Gamma_4 + \Gamma_5$	0.9	Γ_1, Γ_5^*
Nd ³⁺	$4f^3, {}^4I_{9/2}$	$\Gamma_6 + 2\Gamma_8$	-0.7	Γ_8
Pm ³⁺	$4f^4, {}^6I_4$	$\Gamma_1 + \Gamma_3 + \Gamma_4 + \Gamma_5$	-0.8	Γ_1
Sm ³⁺	$4f^5, {}^6H_{5/2}$	$\Gamma_7 + \Gamma_8$	1.0	Γ_8
Eu ³⁺	$4f^6, {}^7F_0$	Γ_1		Γ_1
Tb ³⁺	$4f^7, {}^7F_6$	$\Gamma_1 + \Gamma_2 + \Gamma_3 + \Gamma_4 + 2\Gamma_5$	0.9	Γ_2, Γ_5^*
Dy ³⁺	$4f^8, {}^6H_{15/2}$	$\Gamma_6 + \Gamma_7 + 3\Gamma_8$	0.6	Γ_8
Ho ³⁺	$4f^9, {}^6I_8$	$\Gamma_1 + 2\Gamma_3 + 2\Gamma_4 + 2\Gamma_5$	-0.5	Γ_3^*, Γ_5
Er ³⁺	$4f^{10}, {}^4I_{15/2}$	$\Gamma_6 + \Gamma_7 + 3\Gamma_8$	-0.4	Γ_7
Tm ³⁺	$4f^{11}, {}^3H_6$	$\Gamma_1 + \Gamma_2 + \Gamma_3 + \Gamma_4 + 2\Gamma_5$	0.6	Γ_2^*, Γ_3
Yb ³⁺	$4f^{12}, {}^2F_{7/2}$	$\Gamma_6 + \Gamma_7 + \Gamma_8$	0.7	Γ_7

ELECTRON PARAMAGNETIC RESONANCE AND OPTICAL SPECTRA

A summary of measured paramagnetic resonance g values for trivalent rare-earth ions in various symmetry sites is given in Table II. Additional features of the resonances together with reported optical spectra, estimated crystal-field parameters and energy level structures, and expected resonances spectra for all rare earths are discussed below.

TABLE II. Paramagnetic resonance g values of trivalent rare-earth ions in CaF_2 . Numbers in parenthesis following the g values denote references given in the text.

Rare-earth ion	Cubic ^a	Crystal-field symmetry tetragonal	Trigonal
Ce ³⁺	Γ_8 : 2.00, 3.1±0.1 (34)	$g_{11} = 3.038 \pm 0.003$ (35)	$g_{11} = 2.38 \pm 0.03$ (c)
Nd ³⁺	Γ_7 : 1.297±0.001 (34)(b)	$g_L = 1.396 \pm 0.002$ (35)	$g_L < 0.1$ (c)
Sm ³⁺	See (46)	$g_{11} = 4.412 \pm 0.008$ (5)	
Gd ³⁺	$g = 1.991 \pm 0.002$ (49)	$g_L = 1.301 \pm 0.002$ (5)	
Tb ³⁺		$g_{11} = 0.907 \pm 0.01$ (46)	
Dy ³⁺	Γ_8 : 2.63±0.05 (55)	$g_L = 0.544 \pm 0.15$ (46)	$g_{11} = 1.992 \pm 0.001$ (53)
Er ³⁺	5.48±0.15 (55)	$g_{11} = g_L = 1.992 \pm 0.001$ (52)	$g_{11} = 17.28 \pm 0.01$ (54)
	13.7±0.3 (46)	$g_{11} = 17.768 \pm 0.020$ (54)	$g_L < 0.25$ (54)
	Γ_7 : 7.47±0.03 (56)	$g_L < 0.25$ (54)	(I) $g_{11} = 16 \pm 1$ (55)
	$g = 6.785 \pm 0.002$ (35)	$g_{11} = 1.7 \pm 0.1$ (55)	$g_L < 1$ (55)
		$g_L = 2.82 \pm 0.05$ (55)	(II) $g_{11} = 4.93 \pm 0.05$ (55)
		(I) $g_{11} = 7.76 \pm 0.02$ (35)	$g_L = 1.50 \pm 0.05$ (55)
		$g_L = 6.253 \pm 0.006$ (35)	(I) $g_{11} = 3.30 \pm 0.01$ (59)
		(d) $g_{11} = 6.76 \pm 0.02$ (35)	$g_L = 8.54 \pm 0.02$ (59)
		$g_L = 9.11 \pm 0.01$ (35)	(II) $g_{11} = 2.206 \pm 0.007$ (59)
		(II) $g_{11} = 1.746 \pm 0.002$ (59)	$g_L = 8.843 \pm 0.010$ (59)
		$g_L = 9.16 \pm 0.01$ (59)	
Yb ³⁺	$g = 3.443 \pm 0.002$ (18)	$g_{11} = 2.423 \pm 0.001$ (c)	$g_{11} = 1.323 \pm 0.001$ (65)
	(b)	$g_L = 3.878 \pm 0.001$ (c)	$g_L = 4.389 \pm 0.004$ (65)

^a g values for Γ_8 resonances are for $H \parallel [100]$.

^b See discussion in text.

^c This paper.

^d From excited state at $\sim 24 \text{ cm}^{-1}$.

³² K. W. H. Stevens, Proc. Phys. Soc. (London) **A65**, 209 (1952).

³³ M. Rotenberg, R. Bivins, N. Metropolis, and J. K. Wooten, Jr., *The 3-j and 6-j Symbols* (Technology Press, Massachusetts Institute of Technology, Cambridge, 1959).

Cerium

The cubic crystal-field ground state of Ce^{3+} in CaF_2 should be a Γ_8 quartet. Resonances from an isolated Γ_8 derived from $J = \frac{5}{2}$ would have g values of Λ , $7\Lambda/3$, and $11\Lambda/3$ ($\Lambda = 6/7$ for Ce^{3+}) for a magnetic field $H \parallel [100]$. Dvir and Low³⁴ have reported broad, anisotropic resonances at 4°K and 1.2 cm with $g = 2.00$ and 3.1 ± 0.1 , which were interpreted as due to Ce^{3+} in cubic sites. At high fields a line was observed with $g_{11} = 1.297 \pm 0.001$ and was ascribed to the excited Γ_7 doublet which has a predicted g value of $10/7$. Since the line was seen at 4°K, they conjectured that the cubic-field splitting must be very small, not much larger than the Zeeman energy. As we shall see, however, the cubic field splittings of isolated rare-earth ions in CaF_2 are, in general, very much larger. We have examined several Ce: CaF_2 samples but have not been able to positively identify any cubic-field resonances.

The resonance of Ce^{3+} in sites of tetragonal symmetry has been reported by Baker *et al.*³⁵ The observed g values are derivable from a ground-state doublet of the form $\cos\theta|\pm\frac{5}{2}\rangle - \sin\theta|\mp\frac{3}{2}\rangle$, where $\cos\theta \approx 0.91$. Using this result and the tetragonal field Hamiltonian Eq. (2) yields

$$\tan 2\theta = (2 \times 5^{1/2} B_4^0) / (B_2^0 + 20 B_4^0) = 1.15. \quad (5)$$

This is very close to the cubic field value, $\tan 2\theta = (5)^{1/2}/2 = 1.12$, obtained by setting $B_2^0 = 0$ and $B_4^0 = 5B_4^0$, thereby implying the tetragonal perturbation may be

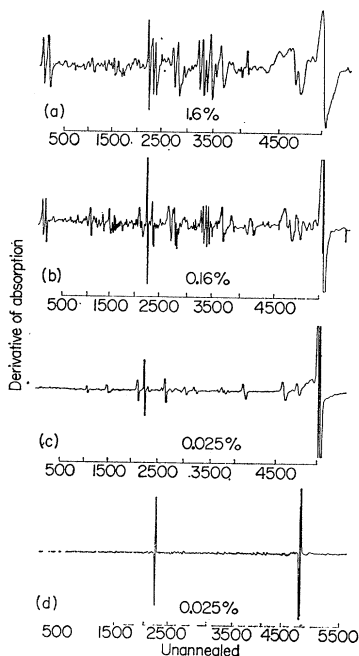


FIG. 2. Paramagnetic resonance spectrum of $\text{Ce}^{3+}:\text{CaF}_2$ at 9.6 kMc/sec and 4.2°K for various Ce concentrations. Spectrum (d) is from an unannealed sample (see text). The magnetic field, in Oe, is approximately $\parallel[100]$.

very small. This, however, is in contradiction to results from other rare earths in CaF_2 , where axial fields arising from nearest-neighbor charge compensation greatly perturb the cubic-field energy level structure. Also no evidence of a small energy level splitting has been found from the spin-lattice relaxation of Ce^{3+} in tetragonal sites.¹ Thus the above agreement may be coincidental, particularly since any admixing from the ${}^2F_{7/2}$ excited state, which should be important for $\text{Ce}^{3+}:\text{CaF}_2$, has been neglected in obtaining this result and since we do not have sufficient information to evaluate B_2^0 , B_4^0 , and B_4^4 separately. The above ground-state wave function and the eigenvalues for $J = \frac{5}{2}$ in a tetragonal field, Eq. (6), are consistent with a case where the second-order crystal-field term does not dominate and $A_2^0 \langle r^2 \rangle$ is positive.

We have observed resonances arising from Ce^{3+} in sites of trigonal symmetry. The g values given in Table II can be compared with those expected for a doublet of the form $|\pm\frac{3}{2}\rangle$ for which $g_{11} = 18/7 = 2.57$, $g_{\perp} = 0$; the differences are probably due mainly to admixing with states from ${}^2F_{7/2}$. The trigonal field eigenvalues for an isolated $J = \frac{5}{2}$ state are given in Eq. (7).

At higher rare-earth impurity concentrations, many additional lines frequently appear in the paramagnetic resonance spectrum as in the case of the optical spectra.²⁷ The increasing spectral complexity with concentration is illustrated in Fig. 2 where three spectra from samples³⁶ containing cerium dopings, each differing by approximately one order of magnitude, are shown. Such additional spectra may be attributed speculatively to the simultaneous existence of several different charge compensation mechanisms and ion arrangements, crystal imperfections, or clusters of ions, but additional work is needed to clarify the situation. The effects of annealing conditions upon the number of lines, linewidth, and line shape is also evident. Traces (a), (b), (c) are from samples which were annealed at 1200°C for 12 h and cooled at a rate of 20°C/h. Trace (d) is from an "as-grown" sample cooled at a rate of $\sim 200^\circ\text{C}/\text{h}$. Note the presence of the two extremely low-field resonances in Figs. 2 (a), (b), which correspond to the zero-field resonances at 9.37 and 9.48 kMc/sec reported by Kaplan.³⁷

The optical spectra of $\text{Ce}^{3+}:\text{CaF}_2$ has been reported by several authors^{34,38-40}; however, no complete crystal-field analysis has been attempted. Whereas the free-ion ${}^2F_{5/2}$ and ${}^2F_{7/2}$ states are separated by 2250 cm^{-1} , the infrared absorption spectrum³⁹ of $\text{Ce}^{3+}:\text{CaF}_2$ is characterized by two broad bands centered around

³⁶ See Ref. 1 for more information on sample preparation.

³⁷ D. E. Kaplan, Bull. Am. Phys. Soc. 8, 468 (1963).

³⁸ P. P. Feofilov, Opt. i. Spektroskopiya 6, 234 (1959) [English transl.: Opt. Spectry. (USSR) 6, 150 (1959)].

³⁹ Z. J. Kiss, Phys. Rev. 127, 718 (1962).

⁴⁰ A. A. Kaplyanskii, V. N. Medvedev, and P. P. Feofilov, Opt. i Spektroskopiya 14, 664 (1963) [English transl.: Opt. Spectry. (USSR) 14, 351 (1963)].

³⁴ M. Dvir and W. Low, Proc. Phys. Soc. (London) 75, 136 (1960).

³⁵ J. M. Baker, W. Hayes, and D. A. Jones, Proc. Phys. Soc. (London) 73, 942 (1959).

2200 and 3200 cm^{-1} . Estimates of the fourth- and sixth-order cubic-field parameters for Ce^{3+} , based upon extrapolations of results for other rare-earth ions in CaF_2 , suggest an x value for ${}^2F_{7/2}$ which in LLW is near the crossing of the Γ_6 and Γ_8 energy levels. Assuming the cubic field is dominant, the above lines could correspond to transitions from the ${}^2F_{5/2}$ Γ_8 ground state to the Γ_6 - Γ_8 and Γ_7 states of ${}^2F_{7/2}$, respectively. At low temperatures several observers have noted a complex line structure about the 2200- cm^{-1} region with a spread $\sim 350 \text{ cm}^{-1}$. In addition to vibrational satellites, this structure could arise from a small Γ_6 - Γ_8 separation or a combination of this and additional splitting of the Γ_8 quartet of ${}^2F_{7/2}$ due to axial crystal fields, since the site symmetries in the samples are not reported.

If one assumes the $\sim 1000 \text{ cm}^{-1}$ spectral separation is due mainly to the cubic-field splitting of ${}^2F_{7/2}$ and equates it to the Γ_7 - Γ_6 energy difference and furthermore assumes $x \approx 0.8$, which is near the Γ_6 - Γ_8 crossover, crystal-field parameters $A_4\langle r^4 \rangle \sim -320 \text{ cm}^{-1}$ and $A_6\langle r^6 \rangle \sim 45 \text{ cm}^{-1}$ are obtained. Using these parameters, an energy separation of $\sim 700 \text{ cm}^{-1}$ is predicted between the Γ_8 and Γ_7 states of ${}^2F_{5/2}$. The above results can only be considered as coarse estimates, however, and may differ greatly from the actual values because, assuming the transitions are assigned correctly: (1) the over-all ${}^2F_{7/2}$ splitting may not be due solely to the cubic field; (2) the x value used was only an estimate; and (3) no account has been made of the off-diagonal elements of the crystal field connecting the ${}^2F_{5/2}$ and ${}^2F_{7/2}$ states. The last is certainly not negligible if the crystal field is as large as estimated above. When the site symmetry and various transitions are established, the crystal-field parameters may be determined by solving the combined spin-orbit and crystal-field problem using a representation in which L_z and S_z are diagonal⁴¹ rather than using the more usual perturbation approach with a $|J, J_z\rangle$ basis.

Praseodymium

The cubic-field ground state of Pr^{3+} in CaF_2 should be either a Γ_1 or a Γ_5 state depending upon the ratio of the fourth- and sixth-order crystal-field parameters. The estimated x value in Table I predicts that the magnetic Γ_5 triplet is lowest. The cubic field wave functions describing the Γ_5 state for $J=4$ are

$$\begin{aligned} & \left(\frac{7}{8}\right)^{1/2} |\pm 3\rangle - \left(\frac{1}{8}\right)^{1/2} |\mp 1\rangle, \\ & \left(\frac{1}{2}\right)^{1/2} (|2\rangle - |-2\rangle). \end{aligned}$$

This state behaves like a spin-1 triplet in a magnetic field yielding an isotropic g value of 2.00.

We have searched for resonances at 9.6 kMc/sec and 2-4°K in a CaF_2 sample containing 0.57% Pr. A weak signal was observed with an isotropic g value ~ 2 which consisted of a single line of width $\sim 20 \text{ G}$ superimposed

upon a broad line of width $\sim 100 \text{ G}$. Hyperfine structure due to the one stable isotope Pr^{147} , nuclear s_z in $I = \frac{5}{2}$, which should be a distinguishing feature was not evident. It was not known whether Pr^{3+} was actually present in sites of cubic symmetry in the sample studied. The absence of a cubic resonance could be due to the difficulty encountered in getting trivalent rare earths belonging to the first half of the $4f$ shell into cubic sites. An additional broad intense resonance corresponding to a zero-field splitting of $\sim 0.3 \text{ cm}^{-1}$ was also observed which is being investigated further.

Neodymium

The cubic-field ground state of Nd^{3+} in CaF_2 is a Γ_8 quartet for all x ($x < 0$). The g values for the Γ_8 resonances depend upon the ratio B_4/B_6 and possible admixing from excited states. A cubic field resonance spectrum for Nd^{3+} : CaF_2 was reported by Vincow and Low⁴²; however, there has been some controversy⁴³ regarding the interpretation of the spectrum which indicates $x \approx -1.0$. In a tetragonal field the ${}^4I_{9/2}$ free-ion ground state is decomposed into five Kramers doublets. Resonances for Nd^{3+} in sites of tetragonal field symmetry were found by Bleaney *et al.*⁵ and fitted to a wave function of the form $a|\pm \frac{3}{2}\rangle + b|\pm \frac{1}{2}\rangle + c|\mp \frac{7}{2}\rangle$ with $c \approx 0$.

The optical absorption and fluorescence spectra of Nd^{3+} in cubic sites have been studied by Kiss.²⁷ The crystal-field parameters determined from the measured splittings of the ${}^4I_{9/2}$ and ${}^4I_{11/2}$ states, neglecting certain off-diagonal terms, are

$$A_4\langle r^4 \rangle = -415 \text{ cm}^{-1}, \quad A_6\langle r^6 \rangle = 33 \text{ cm}^{-1}.$$

Using these results in Eq. (4) yields x values of ≈ -0.70 and ≈ -0.91 for ${}^4I_{9/2}$ and ${}^4I_{11/2}$, respectively. The observed energy level spacings are similar but do not correspond exactly to those in the diagrams of LLW for these x values, thereby indicating that consideration of the admixing of states of different J may be required to determine satisfactory crystal-field parameters. The cubic field energy levels of ${}^4I_{9/2}$ are $\Gamma_8^{(2)} - 0$, $\Gamma_8^{(1)} - 180 \text{ cm}^{-1}$, and $\Gamma_6 - 700 \text{ cm}^{-1}$.

We have examined the fluorescence spectrum⁴⁴ in a CaF_2 sample which, from an examination of the paramagnetic resonance spectrum, had Nd^{3+} predominantly in tetragonal sites. Transitions between ${}^4F_{3/2}$ and ${}^4I_{9/2}$ were observed at 8680, 8750, 8940, 9048, 9078, 9220, and 9465 Å at liquid helium temperatures (these may include vibrational satellites). Lines were also observed at 8860, 9150, and 9335 Å at room temperature which became much smaller or had disappeared at 77°K. In an axial field, the upper fluorescence state ${}^4F_{3/2}$ decomposes into two Kramers doublets separated by $6B_2^0$, where $B_2^0 = \alpha(4f^3, {}^4F_{3/2})A_2^0\langle r^2 \rangle$. If the disappearing lines

⁴² G. Vincow and W. Low, Phys. Rev. **122**, 1390 (1960).

⁴³ W. P. Wolf, J. Phys. Soc. Japan **17**, Suppl. B-I, 442 (1962).

⁴⁴ We thank B. DiBartolo for making these measurements.

⁴¹ M. J. M. Leask, R. Orbach, M. J. D. Powell, and W. P. Wolf, Proc. Roy. Soc. (London) **A272**, 371 (1963).

are caused by thermal depopulation of the upper doublet, this implies a relatively large tetragonal field splitting and an estimated $|A_2^0\langle r^2 \rangle|$ of several hundred cm^{-1} . Such a field would greatly perturb the two Γ_8 quartets of ${}^4I_{9/2}$. Measurements¹ of the spin-lattice relaxation of Nd^{3+} in tetragonal sites indicate an excited state at $\sim 65 \text{ cm}^{-1}$.

Promethium

Neither the paramagnetic resonance nor optical spectrum of $\text{Pm}^{3+}:\text{CaF}_2$, which does not occur naturally, has been reported. In a cubic field the lowest state from 5I_4 is a Γ_1 singlet for all values of x ($x < 0$). The remaining excited states should be relatively far removed.

Samarium

We have searched for resonances at 16 kMc/sec and 4.2°K in an $\sim 0.1\%$ Sm-doped CaF_2 crystal. The sample was prepared so as to enhance the occurrence of trivalent rather than nonresonant divalent samarium ions.⁴⁵ The only resonance observed was one exhibiting tetragonal symmetry about the $[100]$ axes which probably arises from interstitial fluorine charge compensation. The measured g values are $g_{11} = 0.93 \pm 0.04$, $g_{\perp} = 0.57 \pm 0.05$, which can be fitted by an approximate ground doublet wave function $\cos\theta|\pm\frac{5}{2}\rangle - \sin\theta|\mp\frac{3}{2}\rangle$, where $\cos\theta \approx 0.88$. The hyperfine structure of Sm^{147} and Sm^{149} (nuclear spins $I = \frac{7}{2}$) was observed for $H \parallel [100]$ where $A^{147} \approx 170 \times 10^{-4} \text{ cm}^{-1}$. Low⁴⁶ has recently confirmed

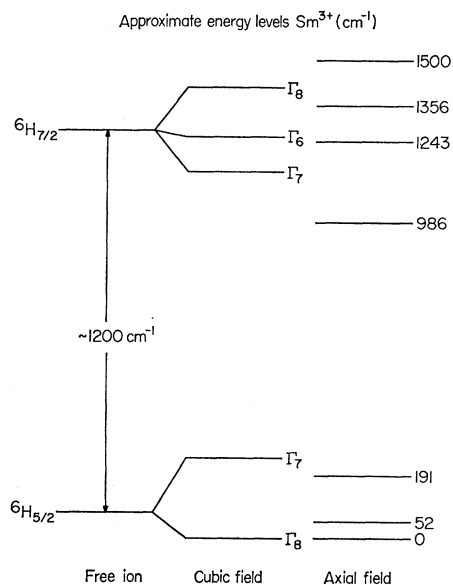


FIG. 3. Crystal-field splitting of the two lowest states of Sm^{3+} in CaF_2 . The cubic-field energy level structure is estimated; the axial field values are from Rabbiner (Ref. 18).

⁴⁵ J. R. O'Connor and H. A. Bostick, *J. Appl. Phys.* **33**, 1868 (1962).

⁴⁶ W. Low, *Phys. Rev.* (to be published).

these measurements and has also reported seeing additional resonances exhibiting cubic and trigonal symmetry; however, their interpretation is not yet complete. In the cubic field of CaF_2 the Sm^{3+} ground state is a Γ_8 quartet.

A complex fluorescence spectrum from Sm^{3+} in a field of axial symmetry in CaF_2 has been observed and analyzed by Rabbiner.¹⁸ The energy levels for ${}^6H_{5/2}$ and ${}^6H_{7/2}$ are shown in Fig. 3. Although no optical spectra of Sm^{3+} in cubic sites have been reported, the ordering of levels within the two lowest 6H states is expected to be approximately as shown (no significance should be attached to the relative energy level spacings, however, which require knowledge of the cubic field parameters and treatment of crystal-field admixing between J states). From Fig. 3 it can be seen qualitatively that the axial field removes the degeneracy of the Γ_8 states and produces a large perturbation on the cubic-field energy level structure. This is also evident from the resonance results where for tetragonal sites $\tan 2\theta$ in Eq. (5) equals 1.46 compared to the cubic-field value of 1.12.

The symmetry of the axial field present in the above fluorescence spectrum was not established. In a tetragonal field, the energies of the three Kramers doublets for an isolated $J = \frac{5}{2}$ state are, from Eq. (2),

$$\begin{aligned} E(\pm\frac{1}{2}) &= -8B_2^0 + 120B_4^0, \\ E(\pm\frac{5}{2}, \mp\frac{3}{2}) &= 4B_2^0 - 20B_4^0 \\ &\quad \pm 6[(B_2^0 + 20B_4^0)^2 + 20(B_4^0)^2]^{1/2}. \end{aligned} \quad (6)$$

In a trigonal field the three doublets from Eq. (3) are

$$\begin{aligned} E(\pm\frac{3}{2}) &= -2B_2^0 - 180B_4^0, \\ E(\pm\frac{5}{2}, \mp\frac{1}{2}) &= B_2^0 + 90B_4^0 \\ &\quad \pm 3[(3B_2^0 - 10B_4^0)^2 + 10(B_4^0)^2]^{1/2}. \end{aligned} \quad (7)$$

These energies are for isolated J states. The crystal-field splitting for $\text{Sm}^{3+}:\text{CaF}_2$ in Fig. 3, however, are not negligible compared to the separations of the various J states. Crystal-field admixing must be taken into account in this case to obtain meaningful parameters B_n^m and predicted g values.

The fluorescence spectrum of Sm^{3+} in a tetragonal field of CdF_2 has also been reported.⁴⁷ Since CdF_2 has (1) an isomorphic lattice structure, (2) a lattice constant very nearly equal to that of CaF_2 , 5.40 Å versus 5.451 Å, and (3) the Pauling ionic radii of Cd^{2+} and Ca^{2+} are approximately equal, 0.97 Å versus 0.99 Å, the crystal-field splittings and ordering of states in the two crystals should be similar. This is indeed found for $\text{Sm}^{3+}:\text{CdF}_2$, where, in place of the energy levels in Fig. 3, the corresponding levels in CdF_2 from ${}^6H_{5/2}$ are at 0, 54, and 147 cm^{-1} and from ${}^6H_{7/2}$ at 959, 1169, 1381, and 1586 cm^{-1} . We shall include data from CdF_2 when similar results for CaF_2 are lacking.

⁴⁷ J. S. Prener and J. D. Kingsley, *J. Chem. Phys.* **38**, 667 (1963).

Europium

The ground state of Eu^{3+} is a singlet 7F_0 . From the fluorescence spectrum of Eu^{3+} in isomorphous CdF_2 , energy levels from the first excited J state 7F_1 are reported⁴⁸ at 307–309 and 400 cm^{-1} . In a crystal field of axial symmetry a $J=1$ state is split into a singlet and a doublet with an energy separation $3\alpha A_2\langle r^2 \rangle$. Setting this equal to the observed 92 cm^{-1} separation and using $\alpha(4f^6, {}^7F_1) = -\frac{1}{5}$, yields $A_2\langle r^2 \rangle \approx 150 \text{ cm}^{-1}$.

Gadolinium

Resonances from Gd^{3+} have been observed in sites of cubic,^{49,50} tetragonal,^{51,52} and trigonal^{10,11,53} symmetry. Since it is an S -state ion, the over-all crystal-field splittings are small, being 0.149 cm^{-1} in a cubic field. In an axial field the ${}^8S_{7/2}$ ground state is split into 4 doublets with a total splitting of about 2 cm^{-1} for tetragonal and trigonal (O_h^-) sites.

Terbium

The cubic-field ground state of $\text{Tb}^{3+}({}^7F_6)$ should be either a Γ_2 singlet or a nonmagnetic Γ_3 doublet, thus no cubic-field resonances are expected nor have they been reported. For $x \lesssim 0.8$, as estimated in Table I, the ground state is a Γ_3 with a relatively near Γ_5 excited state. Terbium resonances and hyperfine structure for ions in sites of tetragonal and trigonal symmetry have been investigated in detail by Forrester and Hempstead.⁵⁴ The resonances for this non-Kramers ion arise from states of principally $|\pm 6\rangle$ character which have a g_{II} of $12\lambda = 18$.

Dysprosium

We have reported⁵⁵ the resonance spectrum of Dy^{3+} in sites of cubic, tetragonal, and trigonal symmetry elsewhere. The cubic-field ground state is a Γ_3 quartet with g values corresponding closely to those calculated from the $J=15/2$ wave functions of LLW for $\Gamma_3^{(1)}$ and $x=0.6$. The first excited state is a Γ_7 doublet located $\sim 8 \text{ cm}^{-1}$ above the ground state. Using this energy separation and the above x value, the cubic-field parameters are $A_4\langle r^4 \rangle = -(200-300) \text{ cm}^{-1}$ and $A_6\langle r^6 \rangle = 30-40 \text{ cm}^{-1}$. The large uncertainty in the values arises from the fact that since we are near the crossover of the Γ_7

and Γ_8 levels and are using the Γ_7 - Γ_8 energy separation as a scale factor, a small change in x can give rise to a large change in the over-all crystal-field splitting of the ground state. Recently, Low⁵⁶ has repeated measurements of the cubic-field spectrum at higher frequency and fields with accordingly more accuracy. He finds $A_4\langle r^4 \rangle = -242 \pm 20 \text{ cm}^{-1}$, $A_6\langle r^6 \rangle = 41 \pm 5 \text{ cm}^{-1}$, where any admixing from ${}^6H_{13/2}$ at $\sim 3500 \text{ cm}^{-1}$ was neglected.

Rabbiner⁵⁷ has reported measurements of the fluorescence spectrum of $\text{Dy}^{3+}:\text{CaF}_2$. The assigned cubic-field splitting of ${}^6H_{15/2}$ is $\approx 615 \text{ cm}^{-1}$ with a Γ_7 ground state and a first excited Γ_8 state at 53 cm^{-1} . The discrepancy with the above may arise from the presence of additional spectral lines from ions in different symmetry sites.

Holmium

The possible cubic-field ground states of Ho^{3+} in CaF_2 are a nonmagnetic $\Gamma_3^{(2)}$ doublet and a $\Gamma_5^{(2)}$ triplet (g value ≈ 5). In the region $0.5 \lesssim x$, where the Γ_3 state is lowest, the first excited state is a $\Gamma_4^{(2)}$ triplet which in the energy level diagram of LLW is nearly coincident with the $\Gamma_3^{(2)}$ doublet.

We have searched for a resonance at X band and 2–4°K in a CaF_2 sample grown by Optovac, Inc., containing a nominal Ho concentration of $\sim 0.1\%$. No resonances were observed. Hayes *et al.*²⁰ have searched for resonances at K band and 4°K in 0.01 and 1% Ho-doped CaF_2 samples which exhibited optical absorption spectra characteristic of Ho^{3+} . Again no resonances were found suggesting the ground state is a Γ_3 state.

Dy^{2+} is isoelectronic with Ho^{3+} . At 77°K the fluorescence spectrum⁵⁸ of Dy^{2+} from 5I_7 to the 5I_8 ground state exhibits a group of lines between 0–100 cm^{-1} and another group around 400–500 cm^{-1} . Laser action has been observed to a terminal state 90 cm^{-1} above the ground state. From an examination of the energy level diagram for $J=8$ in LLW, the above spectrum indicates that $-0.6 < x < -0.4$. Assuming an over-all crystal-field splitting of 450 cm^{-1} for 5I_8 and an x value of -0.5 , yields cubic-field parameters of $A_4\langle r^4 \rangle \sim -400 \text{ cm}^{-1}$ and $A_6\langle r^6 \rangle \sim 40 \text{ cm}^{-1}$ for Dy^{2+} .

Erbium

Resonances from Er^{3+} in sites of cubic,⁵⁵ tetragonal (I)^{55,59} and (II),⁵⁹ and trigonal (I) and (II)⁵⁹ symmetry have been reported. We have examined several CaF_2 crystals at X -band frequencies containing 0.1–1.0% Er and have identified cubic, tetragonal (I) and trigonal (II) resonances. The spectrum at these frequencies and moderately high Er concentrations is complex and consists of many broad, anisotropic lines with overlapping

⁴⁸ J. D. Kingsley and J. S. Prener, Phys. Rev. **126**, 458 (1962).

⁴⁹ W. Low, Phys. Rev. **109**, 265 (1958).

⁵⁰ C. Ryter, Helv. Phys. Acta **30**, 353 (1957).

⁵¹ J. Sierro and R. Lacroix, Compt. Rend. **250**, 2686 (1960).

⁵² V. M. Vinokurov, M. M. Zaripov, Yu. T. Pol'skii, V. G. Stepanov, G. K. Chirkin, and L. Ya. Shekun, Fiz. Tverd. Tela **4**, 2238 (1962) [English transl.: Soviet Phys.—Solid State **4**, 1637 (1963)].

⁵³ V. M. Vinokurov, M. M. Zaripov, Yu. E. Pol'skii, V. G. Stepanov, G. K. Chirkin, and L. Ya. Shekun, Fiz. Tverd. Tela **5**, 599 (1963) [English transl.: Soviet Phys.—Solid State **5**, 436 (1963)].

⁵⁴ P. A. Forrester and C. F. Hempstead, Phys. Rev. **126**, 923 (1962).

⁵⁵ R. W. Bierig and M. J. Weber, Phys. Rev. **132**, 164 (1963).

⁵⁶ W. Low, Proc. Phys. Soc. (London) **76**, 307 (1960).

⁵⁷ N. Rabbiner, Phys. Rev. **132**, 224 (1963); **133**, 1 (1964).

⁵⁸ Z. J. Kiss and R. C. Duncan, Proc. IRE **50**, 1531 (1962).

⁵⁹ U. Ranon and W. Low, Phys. Rev. **132**, 1609 (1963).

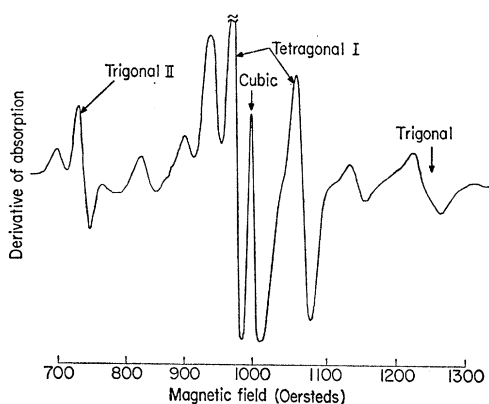


FIG. 4. Low-field portion of the paramagnetic resonance spectrum of $\text{Er}^{3+}:\text{CaF}_2$ arising from ions in cubic, tetragonal, and trigonal crystal fields. Hyperfine structure from Er^{167} ($I = \frac{7}{2}$) is also present. Measurements were made at 9.58 kMc/sec, 4.2°K, and with $H \parallel [110]$.

hyperfine structure, as evident from the low-field portion of the spectrum shown in Fig. 4. Studies of the angular dependence of the spectrum in both the (100) and (111) planes reveal the presence of several unaccounted for resonances which do not correspond to those reported above. One resonance exhibits trigonal symmetry with $g_{11} = 6.31 \pm 0.05$ and $g_{\perp} = 2.14 \pm 0.04$; however, these g values do not satisfy the relationship $(g_{11} + 2g_{\perp}) \approx 3g_{\text{cubic}}(\Gamma_7)$ as do the axial symmetry Er^{3+} resonances observed previously.⁵⁹ The total spectrum was examined with increasing temperature up to $\sim 50^\circ\text{K}$. The trigonal (II) resonance exhibited rapid line broadening in the vicinity of 30°K . The cubic-tetragonal (I) group of lines also exhibited broadening, the cubic line showing the more rapid temperature dependence. By 40°K the cubic and g_{11} , g_{\perp} tetragonal resonances could no longer be distinguished as separate lines. No definite evidence of the tetragonal (I) excited-state resonance reported by Baker *et al.*³⁵ was noted, although it may have been partially masked by other lines in the spectrum. No other excited-state resonances were detected. Measurements¹ of the temperature dependence of T_1 for the trigonal (II) resonance indicate the presence of an excited state at $\sim 50 \text{ cm}^{-1}$.

Paramagnetic resonance studies⁶⁰ have shown that the cubic-field ground state of Ho^{2+} in CaF_2 is a Γ_6 doublet in contrast to the Γ_7 ground state found for isoelectronic Er^{3+} . Since the change in the ratio of the fourth- and sixth-order cubic-field parameters is expected to be small between a divalent ion and its isoelectronic trivalent neighbor, the above result suggests that for both Ho^{2+} and Er^{3+} we are in the vicinity of the crossover of the Γ_6 and Γ_7 levels which for $J = 15/2$ occurs at $x = -0.46$.

The lowest excited crystal-field states in $\text{Ho}^{2+}:\text{CaF}_2$ are⁶¹ a quartet at 30.1 cm^{-1} and a doublet at 33.8 cm^{-1}

⁶⁰ H. R. Lewis and E. S. Sabisky, Phys. Rev. **130**, 1370 (1963).

⁶¹ H. Weakliem and Z. J. Kiss (to be published).

which from LLW suggest an x value ≈ -0.52 . Using these values, the crystal-field parameters for Ho^{2+} are $A_4\langle r^4 \rangle \approx -190 \text{ cm}^{-1}$ and $A_6\langle r^6 \rangle \approx 16 \text{ cm}^{-1}$, where any admixture from ${}^4I_{13/2}$ is probably small and has been neglected. Since x is smaller for Er^{3+} , the sixth-order term must be correspondingly more important.

Pollack⁶² has reported a total separation of about 400 cm^{-1} for the 8 crystal-field levels of ${}^4I_{15/2}$ for Er in an axial field. As an order-of-magnitude estimate, assume a total cubic-field splitting of approximately the same size, 400 cm^{-1} , and an x value of -0.4 . These yield $A_4\langle r^4 \rangle \approx -310 \text{ cm}^{-1}$ and $A_6\langle r^6 \rangle \approx 44 \text{ cm}^{-1}$, which, while not based upon direct spectroscopic data, are, nevertheless, consistent with expected values extrapolated from results for other ions.

Thulium

The cubic-field ground state of Tm^{3+} may be either Γ_2 or Γ_3 . The estimated x value in Table I predicts a Γ_2 singlet lowest. Hayes and Twidell¹⁹ did not observe any resonances in a 0.05% Tm sample at X band and 20°K , but did observe a Tm^{2+} resonance after x irradiation. It has been reported that an axial spectrum of Tm^{3+} has been seen.^{15,63}

Ytterbium

The ground state of Yb^{3+} in cubic sites in CaF_2 is a Γ_7 doublet. The wave function describing the Γ_7 doublet for $J = \frac{7}{2}$ is $(\sqrt{3}/2)|\pm \frac{5}{2}\rangle - (\frac{1}{2})|\mp \frac{3}{2}\rangle$ which yields an isotropic g -value of $24/7 = 3.429$. Low⁶⁴ has measured $g = 3.426 \pm 0.001$; Hayes and Twidell¹⁹ report 3.443 ± 0.002 . We find a g value of 3.441 ± 0.004 . This resonance is observable up to temperatures $\sim 100^\circ\text{K}$, which implied a comparatively long spin-lattice relaxation time.¹

We have also observed resonances due to Yb^{3+} in tetragonal sites. The g values in Table II are consistent with a doublet derived from the cubic Γ_7 , since $(g_{11} + 2g_{\perp}) \approx 3g_{\text{cubic}}(\Gamma_7)$ and indicate that the other states of ${}^2F_{7/2}$ are sufficiently far removed to have little effect on the g values.⁶⁰ They can be fitted by an approximate doublet wave function $0.806|\pm \frac{5}{2}\rangle - 0.591|\mp \frac{3}{2}\rangle$. Two trigonal field resonances have been reported by Low and co-workers.^{21,65}

Kiss³⁹ has investigated the absorption and fluorescence spectrum of isoelectronic Tm^{2+} in CaF_2 . The ${}^2F_{7/2}$ ground state is split into a Γ_7 doublet lowest, a Γ_6 doublet at 547 cm^{-1} , and a Γ_8 quartet at 556 cm^{-1} . The cubic-field parameters derived from these values are $A_4\langle r^4 \rangle = -180 \text{ cm}^{-1}$ and $A_6\langle r^6 \rangle = 35 \text{ cm}^{-1}$, which correspond to an x value of 0.74.

The absorption spectrum of Yb^{3+} was also examined

⁶² S. A. Pollack, Bull. Am. Phys. Soc. **8**, 614 (1963).

⁶³ W. Low, J. Phys. Soc. Japan **17**, Suppl. B-I, 440 (1962).

⁶⁴ W. Low, Phys. Rev. **118**, 1608 (1960); J. Chem. Phys. **37**, 30 (1962).

⁶⁵ W. Low and U. Rosenberger, Compt. Rend. **254**, 1771 (1962).

briefly by Kiss. Two dominant lines were observed at $10\,240\text{ cm}^{-1}$ and $10\,870\text{ cm}^{-1}$, which have also been observed by others.^{28,64,66} If these lines are ascribed³⁹ to transitions to the two cubic-field levels of the ${}^2F_{5/2}$ excited state, an $A_4\langle r^4 \rangle$ value of -280 cm^{-1} is found. Comparing the crystal-field splitting of isoelectronic Tm^{2+} and Yb^{3+} , the larger value for the latter reflects the effect of the additional nuclear charge of the trivalent ion. Approximate cubic-field energy levels for Yb^{3+} , based upon Kiss' assignment and assuming $x \sim 0.7$, are shown in Fig. 5 together with expressions from the eigenvalues. The estimated over-all crystal-field splitting of ${}^2F_{7/2}$ is $\sim 800\text{ cm}^{-1}$.

Low has investigated the electron paramagnetic resonance spectra⁶⁴ and the fine structure in optical spectra^{28,64} of $\text{Yb}:\text{CaF}_2$ and suggested that the cubic field was relatively weak with an over-all ground-state splitting of $\approx 12\text{ cm}^{-1}$. Interpretations based upon such fine structure are, in general, inconsistent with the present results and estimates of the magnitude of the cubic field for other rare-earth ions. The existence of such small splittings for $\text{Yb}:\text{CaF}_2$ are also not evident from measurements of the g value¹⁹ and the rate and temperature dependence of the spin-lattice relaxation.¹ Measurements⁶⁷ of the g shift, temperature dependence, intensity, and infrared absorption of Yb^{3+} in cubic sites in CdF_2 indicate an excited state at $\approx 50\text{--}70\text{ cm}^{-1}$ and an over-all ${}^2F_{7/2}$ splitting of $\approx 116\text{ cm}^{-1}$. We do not understand why these values are so much smaller than those estimated for $\text{Yb}:\text{CaF}_2$. Further work to confirm the measurements and verify the interpretations in the two cases are needed.

The eigenvalues for a $J = \frac{7}{2}$ state in a tetragonal field are given by

$$E(\pm \frac{5}{2}, \mp \frac{3}{2}) = -b_2^0 - 8b_4^0 + 2b_6^0 \pm [(2b_2^0 - 5b_4^0 - 7b_6^0)^2 + 3(5b_4^4 - 7b_6^4)^2]^{1/2}, \quad (8)$$

$$E(\pm \frac{7}{2}, \mp \frac{1}{2}) = b_2^0 + 8b_4^0 - 2b_6^0 \pm [(6b_2^0 - b_4^0 + 3b_6^0)^2 + 35(b_4^4 + 3b_6^4)^2]^{1/2},$$

where

$$\begin{aligned} b_2^0 &= 3B_2^0, & b_6^0 &= 1260B_6^0, \\ b_4^0 &= 60B_4^0, & b_6^4 &= 60B_6^4, \\ b_4^4 &= 12B_4^4, \end{aligned}$$

The observed ground state is of the form $\cos\theta|\pm \frac{5}{2}\rangle - \sin\theta|\mp \frac{3}{2}\rangle$ for which, from Eq. (2) and the doublet wave function found experimentally,

$$\tan 2\theta = \sqrt{3}(5b_4^4 - 7b_6^4)/(2b_2^0 - 5b_4^0 - 7b_6^0) = -3.18. \quad (9)$$

The difference between this value and the cubic-field value $\tan 2\theta = -\sqrt{3}$, corresponding to $b_2^0 = 0$, $b_4^4 = b_4^0$, and $b_6^4 = -b_6^0$, again reveals qualitatively that nearest-

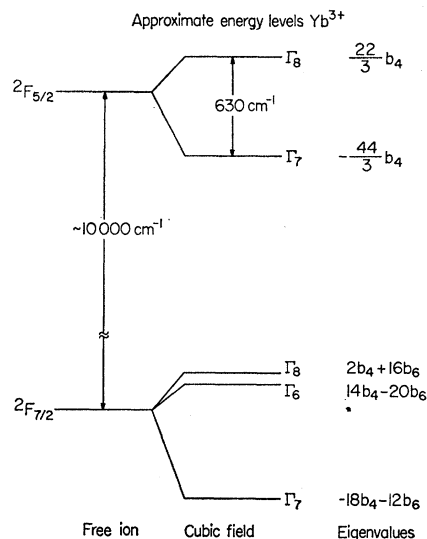


FIG. 5. Estimated cubic-field splitting of Yb^{3+} in CaF_2 , assuming $A_4\langle r^4 \rangle = -280\text{ cm}^{-1}$ and $x = 0.7$.

neighbor charge compensation produces a large change in the crystal field at the trivalent rare-earth site.

CONCLUSIONS

The cubic field in CaF_2 at trivalent rare-earth sites appears to be characterized by parameters in the order of magnitude

$$\begin{aligned} -A_4\langle r^4 \rangle &\sim 250\text{--}430\text{ cm}^{-1}, \\ A_6\langle r^6 \rangle &\sim 30\text{--}45\text{ cm}^{-1}. \end{aligned}$$

The extrapolation of data from divalent ions to the isoelectronic trivalent ions is made subject to two assumptions based upon limited experimental evidence, namely that the ratio of the fourth- and sixth-order parameters of the trivalent ion is in the order of, or less than, that of the divalent ion, and that the trivalent ion parameters are larger than those of the divalent ion. The axial field parameters for nearest-neighbor charge compensation are more difficult to estimate from existing data. The $A_2^0\langle r^2 \rangle$ term, however, probably has a magnitude of several hundred cm^{-1} for both tetragonal (n.n. F^- interstitial) and trigonal (O^{2-}) fields and hence produces a large perturbation on the cubic-field energy levels. The data are usually insufficient to evaluate the A_4^3 , A_4^4 , A_6^3 , and A_6^4 terms for the noncubic crystal fields.

The parameters $A_n^m\langle r^n \rangle$ are expected to vary throughout the rare-earth series. If one assumes the A_n^m 's are constants determined by appropriate lattice sums, then any variation of the crystal-field parameters would be due to $\langle r^n \rangle$. In the early work of Elliott and Stevens,³⁰ this variation was approximated by a multiplicative factor $(Z-55)^{-n/4}$, where Z is the atomic number. Application of this formula has not been universally

⁶⁶ P. P. Feofilov, *Opt. i Spektroskopiya* **5**, 216 (1958).

⁶⁷ P. P. Pashinin and A. M. Prokhorov, *Paramagnetic Resonance* (Academic Press Inc., New York, 1963), p. 197.

successful,⁶⁸ however. This point has been discussed by Freeman and Watson⁶⁹ who, from analyses of data for rare earths in trichlorides and ethylsulfates and using calculated values of the $\langle r^n \rangle$ integrals, conclude that the constancy of A_n^m with Z is not valid.

The data on the cubic-field parameters in CaF_2 for most trivalent ions are too uncertain to derive any explicit variation with Z . Qualitatively, $A_4\langle r^4 \rangle$ appears to exhibit a decrease with increasing Z not unlike that predicted from the variation of Freeman and Watson's $\langle r^4 \rangle$. $A_6\langle r^6 \rangle$, on the other hand, does not show the large, monotonic decrease expected from solely the $\langle r^6 \rangle$ variation, but rather has a moderately constant or slightly increasing value throughout the series. The x values for the trivalent rare earths in cubic sites in CaF_2 given in Table I are estimated by extrapolating the behavior of $A_4\langle r^4 \rangle$ and $A_6\langle r^6 \rangle$. Although these x values must be accepted with considerable reservations, the predicted cubic-field ground states are not inconsistent with available paramagnetic resonance data, and they explain the absence of observed cubic-field resonances for Tb^{3+} , Ho^{3+} , and Tm^{3+} .

APPENDIX: CALCULATION OF CRYSTAL-FIELD MATRIX ELEMENTS USING 3- j AND 6- j SYMBOLS

The crystal-field potential V at a rare-earth ion site can be expanded as

$$V = \sum_{k,q} V_k^q = \sum_{k,q} A_k^q \langle r^k \rangle Y_k^q(\theta, \phi), \quad (\text{A1})$$

where $Y_k^q(\theta, \phi)$ is the spherical harmonic of degree k and azimuthal quantum number q , $\langle r^k \rangle$ is the mean value of the k th power of the $4f$ -electron radius, and the A_k^q 's are parameters related to the strength of the crystal field. Using the concept of operator equivalents, a general term in the crystal-field Hamiltonian may be

rewritten as

$$\zeta_k A_k^q \langle r^k \rangle O_k^q, \quad (\text{A2})$$

where the ζ_k is Stevens' operator equivalent factor³² α, β, γ for $k=2, 4, 6$, respectively, and the O_k^q 's are angular momentum operators, a complete list of which has been given by Orbach.⁷⁰ Tables of matrix elements of these operators within a J manifold and operator equivalent factors for the ground states of the trivalent rare-earth ions are located in various places in the literature. While this approach is convenient for the ground-state computations, when calculating the crystal-field matrix elements of excited states, crystal-field admixing between different J states, and in the treatment of spin-lattice relaxation where all values of k and q may be allowed, the more general approach given below which takes advantage of the tabulated 3- j and 6- j symbols of Rotenberg *et al.*³³ has been useful.

Elliott, Judd, and Runciman⁷¹ have shown how the crystal-field matrix elements of a rare-earth ion in a configuration f^n can be calculated using the tensor operator techniques developed by Racah.⁷² Their expression for the matrix elements of U_q^k , defined as $(4\pi/2k+1)^{1/2} Y_k^q$, rewritten in terms of 3- j symbols ($:::$) and 6- j symbols $\{:::\}$ is

$$\begin{aligned} & \langle f^n WUSLJJ_z | U_q^k | f^n W'U'S'L'J'J'_z \rangle \\ &= \delta(SS') (-1)^{J+S+L'} [(2J+1)(2J'+1)]^{1/2} \\ & \quad \times \begin{pmatrix} J & k & J' \\ -J_z & q & J'_z \end{pmatrix} \begin{Bmatrix} L & J & S \\ J' & L' & k \end{Bmatrix} \\ & \quad \times \langle f^n WUSL || U^k || f^n W'U'S'L' \rangle, \quad (\text{A3}) \end{aligned}$$

where for a rare-earth ion within a given configuration only $k=2, 4, 6$ need be considered. The reduced or double bar matrix element at the end of Eq. (A3) are

TABLE III. Reduced matrix elements of the lowest $S-L$ term of the trivalent rare-earth ions. The first + or - sign corresponds to the first ion of each pair.

Ion	Ground term	$\langle \tau SL U^2 \tau SL \rangle$	$\langle \tau SL U^4 \tau SL \rangle$	$\langle \tau SL U^6 \tau SL \rangle$
Ce^{3+}	2F	± 1	± 1	± 1
Yb^{3+}				
Pr^{3+}	3H	$\pm \frac{1}{3}(11 \times 13/2 \times 7)^{1/2}$	$\mp \frac{2}{3}(13/7)^{1/2}$	$\pm \frac{1}{3}(5 \times 17/7)^{1/2}$
Tm^{3+}				
Nd^{3+}	4I	$\pm (13/2 \times 3 \times 11)^{1/2}$	$\mp (2 \times 13^2 \times 17/3^2 \times 11^2)^{1/2}$	$\pm (5/11)(17 \times 19/3 \times 7)^{1/2}$
Er^{3+}				
Pm^{3+}	6I	$\mp (13/2 \times 3 \times 11)^{1/2}$	$\pm (2 \times 13^2 \times 17/3^2 \times 11^2)^{1/2}$	$\mp (5/11)(17 \times 19/3 \times 7)^{1/2}$
Ho^{3+}				
Sm^{3+}	6H	$\mp \frac{1}{3}(11 \times 13/2 \times 7)^{1/2}$	$\pm \frac{2}{3}(13/7)^{1/2}$	$\mp \frac{1}{3}(5 \times 17/7)^{1/2}$
Dy^{3+}				
Eu^{3+}	7F	∓ 1	∓ 1	∓ 1
Tb^{3+}				

⁶⁸ M. J. D. Powell and R. Orbach, Proc. Phys. Soc. (London) **78**, 753 (1961).

⁶⁹ A. J. Freeman and R. E. Watson, Phys. Rev. **127**, 2058 (1962).

⁷⁰ R. Orbach, Proc. Roy. Soc. (London) **A264**, 458 (1961).

⁷¹ J. P. Elliott, B. R. Judd, and W. A. Runciman, Proc. Roy. Soc. (London) **A240**, 509 (1957).

⁷² G. Racah, Phys. Rev. **62**, 438 (1942); **63**, 367 (1943).

TABLE IV. Normalization factors N_{k^q} for Eq. (A4). Numbers in column F are multiplicative factors common to all elements in the row. Other column headings denote q values.

N_{k^q}	F	0	1	2	3	4	5	6
N_{2^q}	$-4(7/3 \times 5)^{1/2}$	1	$1/(2 \times 3)^{1/2}$	$1/2(2 \times 3)^{1/2}$				
N_{4^q}	$8(2 \times 7/11)^{1/2}$	1	$1/4(5)^{1/2}$	$1/2(2 \times 5)^{1/2}$	$1/4(5 \times 7)^{1/2}$	$1/(2 \times 5 \times 7)^{1/2}$		
N_{6^q}	$-160(7/3 \times 11 \times 13)^{1/2}$	1	$1/2(2 \times 3 \times 7)^{1/2}$	$1/(3 \times 5 \times 7)^{1/2}$	$1/2(3 \times 5 \times 7)^{1/2}$	$1/3(2 \times 7)^{1/2}$	$1/6(7 \times 11)^{1/2}$	$1/(3 \times 7 \times 11)^{1/2}$

tabulated in Table III for the lowest L - S term of the trivalent rare-earth ions, where τ denotes the remaining quantum numbers required to specify the state. Many of the reduced matrix elements for the various ions are related by simple multiplicative factors derivable from the relationships discussed by Judd.⁷³ The reduced matrix elements of U^k for other L - S terms may be calculated using Racah's fractional parentage coefficients as shown by Elliott, Judd, and Runciman. Nielson and Koster⁷⁴ have recently tabulated these matrix elements for f^n configurations.

In Stevens' operator equivalence approach, certain normalization factors have been absorbed into the definition of the A_{k^q} . Thus if Eq. (A3) is used to evaluate crystal-field parameters and the A_{k^q} 's are to be compared with those derived elsewhere using operator

⁷³ B. R. Judd, Proc. Roy. Soc. (London) **A250**, 562 (1959).
⁷⁴ C. W. Nielson and George F. Koster, *Spectroscopic Coefficients for the p^n , d^n , and f^n Configurations*, (The M.I.T. Press, Massachusetts Institute of Technology, Cambridge, 1963).

equivalent factors, then (A2) should be replaced by

$$N_{k^q} A_{k^q} \langle r^k \rangle U_q^k. \tag{A4}$$

The normalization factors N_{k^q} for the various k 's and q 's are listed in Table IV.

In terms of the 6- j symbols, the operator equivalent factors, ζ_k , for different J states are related by

$$\frac{\langle SLJ' || \zeta_k || SLJ' \rangle}{\langle SLJ || \zeta_k || SLJ \rangle} = (-1)^{J'-J} \frac{2J'+1}{2J+1} \times \left[\frac{(2J'-k)!(2J+k+1)!}{(2J-k)!(2J'+k+1)!} \right]^{1/2} \times \left\{ \begin{matrix} J' & J' & k \\ L & L & S \end{matrix} \right\} / \left\{ \begin{matrix} J & J & k \\ L & L & S \end{matrix} \right\}, \tag{A5}$$

where $k=2, 4, 6$ correspond to α, β, γ , respectively.